Transverse Elastic Modulus of Tobacco Mosaic Virus Superlattice

X. Wang[*,**], and H. Wang[*]

[*] Department of Mechanical Engineering, North Dakota State University, Fargo, ND 58108. USA, xinnan.wang@ndsu.edu

[**] Materials and Nanotechnology Graduate Program, North Dakota State University, Fargo, ND 58108. USA, haoran.wang@my.ndsu.edu

ABSTRACT

Mechanical properties of tobacco mosaic virus superlattice nanorodes were measured by nanoindentation with an atomic force microscope (AFM) probe. The elastic modulus of TMV superlattice was measured from the AFM force-displacement curves. The extended JKR model was proposed by processing both the theoretical model and the experimental data to obtain the transverse elastic modulus.

Keywords: TMV, superlattice, mechancical property, elastic modulus, JKR model

INTRODUCTION

Tobacco mosaic virus (TMV) was discovered over a century ago, [1] and recently it has recently been emerged and utilized as a major template for the synthesis of functional materials at micro or nanoscale. [2] TMV consists of 2130 protein subunits that are positioned helically around an RNA, resulting in a 300 nm long thick tubular structure with an outer radius of 9 nm and an inner radius of 2 nm. [3] Its popularity in organic syntheses as the nanotemplate is largely due to its superb structural and functionalized surficial stability in a broad range of thermal and chemical conditions. [4] One of the intriguing features of TMV is its natural linear self-assembly up to several tens of microns, making it an attractive biotemplate for the synthesizing novel organic, inorganic and metallic one-dimensional (1D) nanomaterials. [5] Such kind of 1D materials have already been used in nanoelectronic applications. [6]

Real applications of the synthesized nano biomaterials [7] highly depend upon acquisition of their physical properties of the biotemplates as well as the final materials. Particularly, understanding of the mechanical properties of such materials is key in pushing their applications forward in nanotechnology. Atomic force microscopy (AFM) has been widely accepted as a powerful tool in probing the mechanical properties of bio-nanoparticles and investigate the particle-substrate interactions. [8]

Very recently, a 2-D hexagonally-packed rod-like TMV superlattice of tens of micrometers in length has been synthesized by mixing TMV solution with Ba^{2+}. [9] It is important to study the mechanical properties of such 1D superlattice for its potential utilization as functional materials and devices. In this contribution, the mechanical properties of TMV/Ba^{2+} superlattice are reported using AFM-based nanoindentation and the finite element analysis of the indentation at two radial directions, to compare the mechanical properties with that of the individual constituent materials.

MATERIALS AND METHODS

The TMV superlattice solution was obtained from the mixture of the $BaCl_2$ and TMV solution (molar ratio of TMV: Ba^{2+} = 1: 9.2×10^4) and diluted with deionized water (volume ratio 1:1). Detailed synthesis procedure can be found in reference [9]. A drop of solution on a Si wafer was centrifuged to generate mono-layer dispersion, and was dried for 30 min under ambient conditions (40% R.H., 21 ^{o}C) for AFM (Brukers D3100) observation and mechanical testing. The superlattice sample prior to dilution was also analyzed using a field emission scanning electron microscope (FESEM, Hitachi S4700).

For the measurement of elastic modulus of the superlattice and study of deformation behavior, firstly AFM (AFM probe: Tap150-G, Nanoandmore, tip radius: 12 nm) was used to image scan and locate individual superlattice rods, followed by *in situ* indentation. For a typical indentation, the relative displacement between the tip and sample surface was less than 4 nm, therefore the tip was simplified to be a sphere. The indentation was performed at 10 different locations with an speed of 185 nm/s. The corresponding normal force *v.s.* AFM Z piezo displacement (F-DISP) curve was recorded for elastic modulus analysis.

The indentation force was converted from the deflection of the AFM probe cantilever, whose spring constant k_c needed to be measured. In the study, Sader method was adopted, where k_c is given by

$$k_c = M_e \rho_c b h l \omega_{vac}^2 \quad (1)$$

where M_e is the normalized effective mass which is 0.242, [10] ρ_c is the density of the Si cantilever, ω_{vac} is the unloaded resonance frequency in vacuum, and h, b, and l are the thickness, width and length, respectively.

RESULTS AND DISCUSSION

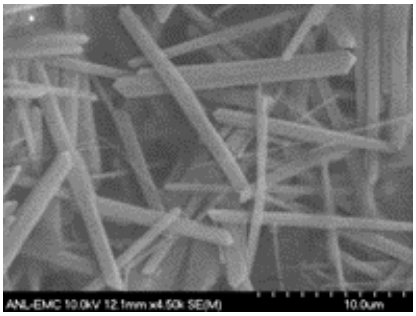

Figure 1: FESEM of TMV/Ba^{2+} superlattice rods.

FESEM observation in Figure 1 shows the TMV superlattice rodes. These rod-like particles were of tens of microns' length and several microns' width, and were formed by Ba^{2+}.

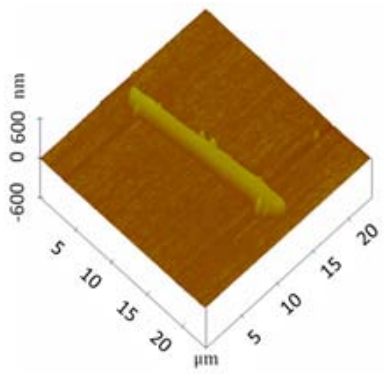

Figure 2: AFM height image of a superlattice.

Figure 2 shows the AFM height image of a representative TMV superlattice. The superlattice is 19.18 μm in length, and width of 1.5 μm, which is in good agreement with the FESEM observation. Since the Z piezo displacement after the tip-sample contact was the inclusion of the sample deformation and the cantilever deflection. To extract the sample deformation, indentations were also performed directly on the Si substrate. [12] Thus, the force *v.s.* indentation depth (F-Δz) relationship was obtained for elastic modulus analysis. Figure 3 is the plot of the retraction F-DISP curves of the sample and Si wafer. The distance Δz is the nominal indentation depth on the sample.

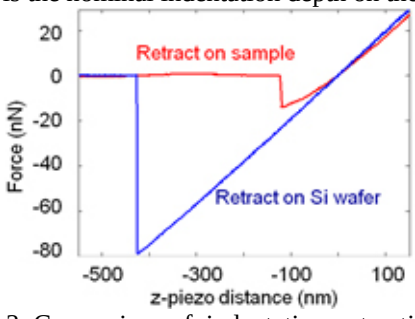

Figure 3: Comparison of indentation retraction F-D curves on Si wafer and superlattice.

To obtain the elastic modulus, the JKR model was modified due to the fact that the probe tip had a radius of 12 nm, which required a smaller indentation depth to fit into this model. Hence, the indentation depth δ and the load P can be given as:

$$\delta = \frac{a}{2}\ln\frac{R+a}{R-a} - \sqrt{\frac{8\pi aG}{3K}} \tag{2}$$

$$P = \frac{3aK}{2}\left(\frac{R^2+a^2}{4a}\ln\frac{R+a}{R-a} - \frac{R}{2} - \sqrt{\frac{8\pi aG}{3K}}\right) \tag{3}$$

where a is the contact radius; the nominal elastic constant; K is calculated by

$$K = \frac{4}{3\pi(k_1+k_2)} \tag{4}$$

where $k_1 = \frac{1-\nu_1^2}{\pi E_1}$ and $k_2 = \frac{1-\nu_2^2}{\pi E_2}$, ν_1, ν_2 and E_1, E_2 are the Poisson's ratio and elastic moduli of the two spheres, respectively; G is the adhesion release rate at the contact surfaces, which is determined by

$$G = -\frac{6P_0}{5\pi R} \tag{5}$$

where P_0 is the pull-off force; the nominal radius R is obtained by the equation

$$R = \frac{R_i R_s}{R_i + R_s} \tag{6}$$

where R_i and R_s represent the radii of the indenter and sample in contact respectively. The adhesion force from the indentation results is ~14 nN. The equivalent radius R is approximated to be $R_i = 12$ nm, as the radius of the superlattice is much bigger that the tip radius. The Poisson's ratio of the superlattice is assumed 0.38, commonly used for biological materials.

The experimental and theoretical Force *v.s.* Depth (F-DEP) curves based on equations (2) and (3) is plotted in FIG. 4. The elastic modulus was calculated to be 2.14 GPa.

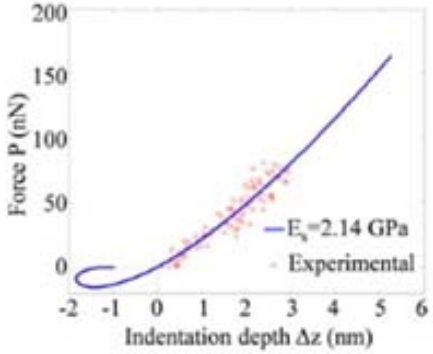

Figure 4: Comparison of indentation retraction F-D curves on Si wafer and superlattice

CONCLUSIONS

AFM based nanoindentation was used to evaluate the transverse elastic modulus of TMV superlattice formed by TMV in Ba^{2+} solution. Based on the experimental F-DEP curves, extended JKR model was utilized to extract the elastic modulus of the superlattice sample. An elastic modulus of 2.14 GPa was obtained.

ACKNOWLEDGEMENTS

Funding support is provided by ND NASA EPSCoR FAR0017788, and NDSU Development Foundation FAR0017503. We are thankful for Dr. Tao Li and Byeongdu Lee for providing the FESEM images at Argonne National Lab.

REFERENCES

[1]. (a) Craeger, A. N.; Scholthof, K. B.; Citovsky, V.; Scholthof, H. B., Tobacco mosaic virus: pioneering research for a century. Plant Cell 1999, 11 (3), 301-308; (b) Harrion, D.; Wilson, T. M. A., Milestones in the research on tobacco mosaic virus. Philosophical transactions of the Royal Society of London. Series B, Biological sciences. 1999, 354 (1383), 521-529.

[2]. (a) Dujardin, E.; Peet, C.; Stubbs, G.; Culver, N. J.; Mann, S., Organization of metallic nanoparticles using tobacco mosaic virus templates. Nano Lett. 2003, 3 (3), 413-417; (b) Shenton, W.; Douglas, T.; Young, M.; Stubbs, G.; Mann, S., Inorganic-Organic Nanotube Composites from Template Mineralization of Tobacco Mosaic Virus. Advanced Materials 1999, 11, 253-256; (c) Fowler, C. E.; Shenton, W.; Stubbs, G.; Mann, S., Tobacco mosaic virus liquid crystals as templates for the interior design of silica mesophases and nanoparticles. Adv. Mater. (Weinheim, Ger.) 2001, 13, 1266-1269; (d) Huang, J.; Kaner, R. B., Nanofiber Formation in the Chemical Polymerization of Aniline: A Mechanistic Study. Angewandte Chemie International Edition 2004, 43, 5817-5821.

[3]. Klug, A., The tobacco mosaic virus particle: structure and assembly. Philosophical Transactions: Biological Sciences 1999, 354, 531-535.

[4]. (a) Kausche, G. A., Über eine Trennungsmöglichkeit von Mischviren auf Grund ihrer differenten PH-Stabilität. Naturwissenschaften 1938, 26 (14), 219-219; (b) Wadu-Mesthrige, K.; Pati, B.; McClain, W. M.; Liu, G.-Y., Disaggregation of Tobacco Mosaic Virus by Bovine Serum Albumin. Langmuir 1996, 12, 3511-3515.

[5]. (a) Fonoberov, V. A.; Balandin, A. A., Phonon confinement effects in hybrid virus-inorganic nanotubes for nanoelectronic applications. Nano Lett. 2005, 5 (10), 1920-1923; (b) Royston, E.; Lee, S. Y.; Culver, J. N.; Harris, M. T., Characterization of silica-coated tobacco mosaic virus. J. Colloid Interface Sci. 2006, 298 (2), 706-712; (c) Knez, M.; Bittner, A. M.; Boes, F.; Wege, C.; Jeske, H.; Maiss, E.; Kern, K., Biotemplate synthesis of 3-nm nickel and cobalt nanowires. Nano Lett. 2003, 3 (8), 1079-1082; (d) Knez, M.; Kadri, A.; Wege, C.; Gosele, U.; Jeske, H.; Nielsch, K., Atomic layer deposition on biological macromolecules: Metal oxide coating of tobacco mosaic virus and ferritin. Nano Lett. 2006, 6 (6), 1172-1177; (e) Knez, M.; Sumser, M.; Bittner, A. M.; Wege, C.; Jeske, H.; Martin, T. P.; Kern, K., Spatially selective nucleation of metal clusters on the tobacco mosaic virus. Adv. Funct. Mater. 2004, 14 (2), 116-124; (f) Knez, M.; Sumser, M. P.; Bittner, A. M.; Wege, C.; Jeske, H.; Hoffmann, D. M. P.; Kuhnke, K.; Kern, K., Binding the tobacco mosaic virus to inorganic surfaces. Langmuir 2004, 20 (2), 441-447; (g) Lee, S. Y.; Culver, J. N.; Harris, M. T., Effect of CuCl2 concentration on the aggregation and mineralization of Tobacco mosaic virus biotemplate. J. Colloid Interface Sci. 2006, 297 (2), 554-560.

[6]. Tseng, R. J.; Tsai, C.; Ma, L.; Ouyang, J.; Ozkan, C. S.; Yang, Y., Digital memory device based on tobacco mosaic virus conjugated with nanoparticles. Nat Nano 2006, 1 (1), 72-77.

[7]. (a) Kalinin, S. V.; Jesse, S.; Liu, W. L.; Balandin, A. A., Evidence for possible flexoelectricity in tobacco mosaic viruses used as nanotemplates. Appl. Phys. Lett. 2006, 88 (15); (b) Fonoberov, V. A.; Balandin, A. A., Low-frequency vibrational modes of viruses used for nanoelectronic self-assemblies. Physica Status Solidi B-Basic Research 2004, 241 (12), R67-R69.

[8]. (a) Malkin, A. J.; Land, T. A.; Kuznetsov, Y. G.; McPherson, A.; Deyoreo, J. J., Investigation of virus crystal-growth mechanisms by in-situ atomic-force microscopy. Phys. Rev. Lett. 1995, 75 (14), 2778-2781; (b) Wadu-Mesthrige, K.; Pati, B.; McClain, W. M.; Liu, G. Y., Disaggregation of Tobacco Mosaic Virus by Bovine Serum Albumin. Langmuir 1996, 12 (14), 3511-3515; (c) Fang, J. Y.; Knobler, C. M.; Gingery, M.; Eiserling, F. A., Imaging bacteriophage T4 on patterned organosilane monolayers by scanning force microscopy. J. Phys. Chem. B 1997, 101 (43), 8692-8695; (d) Maeda, H., An atomic force microscopy study for the assembly structures of tobacco mosaic virus and their size evaluation. Langmuir 1997, 13 (15), 4150-4161; (e) Kuznetsov, Y. G.; Malkin, A. J.; Lucas, R. W.; Plomp, M.; McPherson, A., Imaging of viruses by atomic force microscopy. J. Gen. Virol. 2001, 82, 2025-2034; (f) Suci, P. A.; Klem, M. T.; Douglas, T.; Young, M., Influence of electrostatic interactions on the surface adsorption of a viral protein cage. Langmuir 2005, 21 (19), 8686-8693; (g) Ivanovska, I. L.; de Pablo, P. J.; Ibarra, B.; Sgalari, G.; MacKintosh, F. C.; Carrascosa, J. L.; Schmidt, C. F.; Wuite, G. J. L., Bacteriophage capsids: Tough nanoshells with complex elastic properties. Proc. Natl. Acad. Sci. U. S. A. 2004, 101 (20), 7600-7605; (h) Michel, J. P.; Ivanovska, I. L.; Gibbons, M. M.; Klug, W. S.; Knobler, C. M.; Wuite, G. J. L.; Schmidt, C. F., Nanoindentation studies of full and empty viral capsids and

the effects of capsid protein mutations on elasticity and strength. Proc. Natl. Acad. Sci. U. S. A. 2006, 103 (16), 6184-6189; (i) Zhao, Y.; Mahajan, N.; Long, S.; Wang, Q.; Fang, J., Stability of virus nanoparticles on substrates under applied load with atomic force microscope. Micro & Nano Letters 2006, 1 (1), 1-4.
[9]. Li, T.; Winans, R. E.; Lee, B., Superlattice of Rodlike Virus Particles Formed in Aqueous Solution through Like-Charge Attraction. Langmuir 2011, 27 (17), 10929-10937.
[10]. Sader, J. E.; Larson, I.; Mulvaney, P.; White, L. R., Method for the calibration of atomic force microscope cantilevers. Rev. Sci. Instrum. 1995, 66 (7), 3789-3798.
[11. Johnson, K. L., Contact Mechanics. 1992, 84-106.
[12]. Wang, X. N.; Niu, Z. W.; Li, S. Q.; Wang, Q.; Li, X. D., Nanomechanical characterization of polyaniline coated tobacco mosaic virus nanotubes. Journal of Biomedical Materials Research Part A 2008, 87A (1), 8-14.